Structural properties of $Bi_{1-x}La_xFeO_3$ studied by micro-Raman scattering*

Yang Yang(杨 洋)[a], Liu Yu-Long(刘玉龙)[a]†, Zhu Ke(朱 恪)[a], Zhang Li-Yan(张丽艳)[a], Ma Shu-Yuan(马树元)[b], Liu Jie(刘 洁)[c], and Jiang Yi-Jian(蒋毅坚)[c]

[a] *Institute of Physics, Chinese Academy of Sciences, Beijing* 100190, *China*
[b] *College of Physical Science and Technology, Guangxi University, Nanning* 530004, *China*
[c] *College of Laser Engineering, Beijing University of Technology, Beijing* 100124, *China*

(Received 2 April 2009; revised manuscript received 8 July 2009)

This paper reports that La-doped $BiFeO_3$ ($Bi_{1-x}La_xFeO_3$, x = 0, 0.1, 0.2, 0.3, 0.6, 0.8 and 1.0) were studied by using micro-Raman spectroscopy and x-ray diffraction (XRD). The XRD patterns indicate that the structure of $Bi_{1-x}La_xFeO_3$ changes from rhombohedral $BiFeO_3$ to orthorhombic $LaFeO_3$. The results of Raman spectroscopy show good agreement with the XRD results. Strikingly, the phonon peak at around 610 cm^{-1} and the two-phonon peaks in the high frequency range exist in all compounds and enhance with increasing La substitution. The increasing intensity of the 610 cm^{-1} peak is attributed to the changes in the FeO_6 octahedron during the rhombohedral–orthorhombic phase transition. The enhancements of the two-phonon peaks are associated with the breakdown of the cycloid spin configuration with the appearance of the orthorhombic structure. These results indicate the existence of strong spin–phonon coupling in $Bi_{1-x}La_xFeO_3$, which may provide useful information for understanding the effects of La content on the structural and magnetic properties of $Bi_{1-x}La_xFeO_3$.

Keywords: $Bi_{1-x}La_xFeO_3$, Raman scattering, phase transition, spin–phonon coupling

PACC: 7830G, 7550E

1. Introduction

Magnetoelectric (ME) multiferroics have attracted much attention in past years because of their basic physical properties and potential applications in data storage, spintronics and quantum electomagnets.[1−3] Bismuth ferrite ($BiFeO_3$) is one of the most intensively studied multiferroic materials since it exhibits simultaneously antiferromagnetic (T_N = 643 K) and ferroelectric (T_C = 1103 K) properties at room temperature.[4] The ferroelectric state is realized by a large displacement of the Bi ions relative to the FeO_6 octahedra. The ferroelectric polarization lies along the pseudocubic ⟨111⟩ direction, leading to the formation of eight possible polarization variants. On the other hand, $BiFeO_3$ exhibits G-type antiferromagnetic ordering, in which the Fe magnetic moments are aligned ferromagnetically within the (111) plane and antiferromagnetically between the adjacent (111) planes. Additionally, the spin configuration is modulated by a long-range cycloid structure (620 Å periodicity, 1 Å=0.1 nm) in the bulk, and the preferred orientation of the antiferromagnetically aligned spins is in the (111) plane, which is perpendicular to the ferroelectric polarization direction with six equivalent easy axes within that plane.[5] Various experimental and theoretical methods have been carried out for studying the coupling between these two orderings of this material for basic physical and applied reasons.[6−13] It has been evidenced that the multiferroic properties of $BiFeO_3$ have been significantly enhanced by substitution with non-ferroelectric end member $LaFeO_3$ or by the strain in the film form.[11−15] By La-doping, $BiFeO_3$ has achieved the properties necessary for fatigue-free ferroelectric switching, excellent dielectric loss, enhanced remanent polarization and magnetization. In recent years, increasing attention has been paid to La-doped $BiFeO_3$ films because of their future applications in nonvolatile ferroelectric random access memories (FeRAMs) and spintronic devices. However, most of those works focused on $Bi_{1-x}La_xFeO_3$ materials with low La substitution ($x \leq 0.2$). Moreover, the strain arising from the lattice mismatch between the film and the substrate inhibits us from understanding precisely the effect of La content on the electrical and magnetic properties of $Bi_{1-x}La_xFeO_3$ materials

*Project supported by the National Natural Science Foundation of China (Grant Nos. 10674171 and 10874236).
†Corresponding author. E-mail: ylliu@aphy.iphy.ac.cn
© 2010 Chinese Physical Society and IOP Publishing Ltd

as well as their structure. Therefore, it is crucial to further investigate the structure of $Bi_{1-x}La_xFeO_3$ to gain more information about the origin of the superior properties as well as the applications in the future.

Raman spectroscopy has been proved to be a convenient method to study the elementary excitations and their interaction in solid state materials.[16−30] Although $BiFeO_3$ materials in various forms have been extensively studied by Raman scattering extensively in recent years,[16−22] reports on the Raman studies of $Bi_{1-x}La_xFeO_3$, especially for those with high La content, are limited. In this paper, we report a systematic Raman study of $Bi_{1-x}La_xFeO_3$ with x ranging from 0 to 1.0. Both XRD and Raman results indicated that the structure of $Bi_{1-x}La_xFeO_3$ changes from rhombohedral $BiFeO_3$ to orthorhombic $LaFeO_3$. The Raman mode at around 610 cm^{-1} and the two-phonon modes show obvious enhancement with increasing La content, indicating the strong spin–phonon coupling in $Bi_{1-x}La_xFeO_3$. Our results suggest that Raman spectroscopy would be a useful tool for investigating the structural and magnetic properties of iron oxides.

2. Experimental details

The $Bi_{1-x}La_xFeO_3$ ($x = 0$, 0.1, 0.2, 0.3, 0.6, 0.8 and 1.0) powders are prepared by a molten salt synthesis (MSS) method, which has been reported in detail in another article recently.[31] The crystal structure of the samples was examined by an x-ray diffractometer with a Cu Kα radiation source. The Raman spectra were measured in backscattering configuration by using a micro-Raman spectrometer (Horiba/Jobin Yvon HR800). A 50× microscope objective lens was used in order to focus the laser beam and collect the scattered light. A laser line with 532 nm wavelength was used as the excitation source, and the laser power was kept at < 0.5 mW to prevent laser-induced damage to the sample. All the measurements were carried out at room temperature.

3. Results and discussions

Figure 1 displays the XRD patterns for the $Bi_{1-x}La_xFeO_3$ samples. As shown from the measured XRD patterns, all samples exhibit a single-phase perovskite structure with no trace of other impurity phases (e.g. Fe_2O_3, Bi_2O_3, La_2O_3, $Bi_2Fe_4O_9$, $Bi_{25}FeO_{39}$, etc) detected. As shown in Fig. 1, the structure of $Bi_{1-x}La_xFeO_3$ evolves from the rhombohedral ($R3c$) phase to the orthorhombic ($Pnma$) phase, which is revealed clearly from further detailed analysis of some diffraction peaks. For example, the (006) diffraction peak, which is assigned as the index of the rhombohedral structure in $BiFeO_3$, becomes weak with increasing La content and disappears at $x = 0.60$, as shown in Fig. 1(b). The disappearance of the (006) peak indicates the structural transition from the rhombohedral phase to the orthorhombic phase at $x = 0.60$. In addition, broadening and merging of diffraction peaks are observed when increasing La content from $x = 0$ to 0.3, especially in the XRD curve for $x = 0.3$.

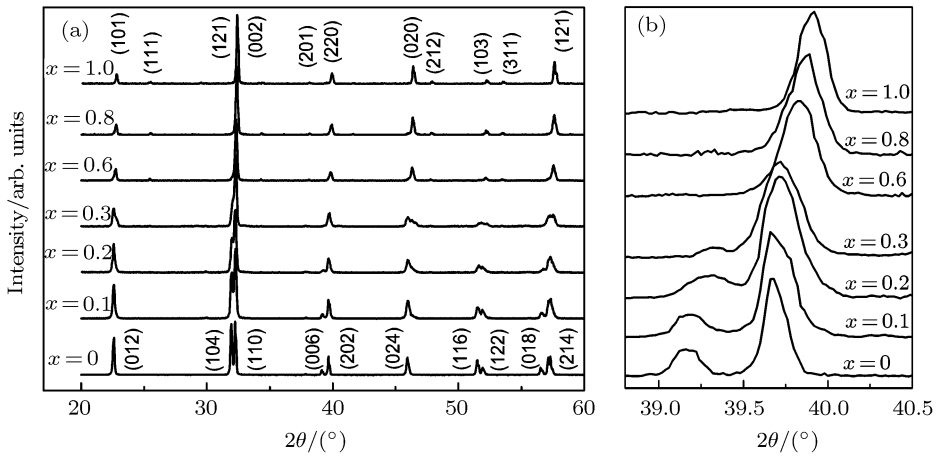


Fig. 1. (a) The XRD patterns of $Bi_{1-x}La_xFeO_3$ with $x = 0$, 0.1, 0.2, 0.3, 0.6, 0.8 and 1.0. (b) The magnified view of the peak in the 2θ range 38.5°–40.5°.

Such a phenomenon suggests that the largest lattice distortion and defects exist in $Bi_{0.7}La_{0.3}FeO_3$, resulting from the drastic competition between the rhombohedral and orthorhombic symmetries. However, from then on, the bandwidths of diffraction peaks decrease gradually with further increase of the La content, indicating that the structure has been improved greatly. This is attributed to the case that the orthorhombic structure becomes dominant in these compounds. When $x = 0.8$ and 1.0, $Bi_{1-x}La_xFeO_3$ is completely in the orthorhombic phase, as illustrated by the XRD patterns.

According to group theory, pure $BiFeO_3$ with rhombohedral $R3c$ structure has 13 Raman-active modes: $4A_1+9E$, while pure $LaFeO_3$ with orthorhombic $Pnma$ structure has 21 Raman-active modes: $7A_g+2B_{1g}+7B_{2g}+5B_{3g}$. The structural transition in $Bi_{1-x}La_xFeO_3$ samples would be easily detected through Raman spectroscopy because of the large discrepancy between the numbers of Raman-active modes of these two structures.

Figure 2 presents the Raman spectra of $Bi_{1-x}La_xFeO_3$ powders with $x = 0$, 0.1, 0.2, 0.3, 0.6, 0.8 and 1.0, which show obvious changes with increasing La content. According to the variations of the first order Raman peaks below 800 cm^{-1}, these spectra can be separated into three groups. One group with the La concentration of up to 20% resembles the vibration modes of the nondoped $BiFeO_3$. Three strong peaks at 140, 172, and 217 cm^{-1} and nine weak peaks at 262, 275, 307, 345, 369, 429, 470, 521, and 610 cm^{-1} can be seen in these three spectra, which are consistent with previous work.[17−20] In accordance with studies on structurally related compounds, the 610 cm^{-1} peak is assigned as a symmetric oxygen breathing mode. In addition, three broad bands in the range of 900–1300 cm^{-1} are observed clearly, which are attributed to the two-phonon peaks.[21] It is noteworthy that the intensities of the two-phonon peaks are much lower than those of their corresponding first order phonons, which has been attributed to the strong spin-two-phonon coupling in $BiFeO_3$.[21,22] Moreover, the frequency shifts of the second order peaks are slightly lower than twice the frequency shifts of the corresponding first order peaks. Such downshifts are associated with the asymmetry of the anharmonic potential of the system.[24] All these spectral features suggest that the low-doped $Bi_{1-x}La_xFeO_3$ ($x \leq 0.2$) is still in the rhombohedral phase. Comparing these three spectra, we can see clearly that both the first-order phonon modes and the two-phonon modes exhibit blueshift and broadening with increasing La content.

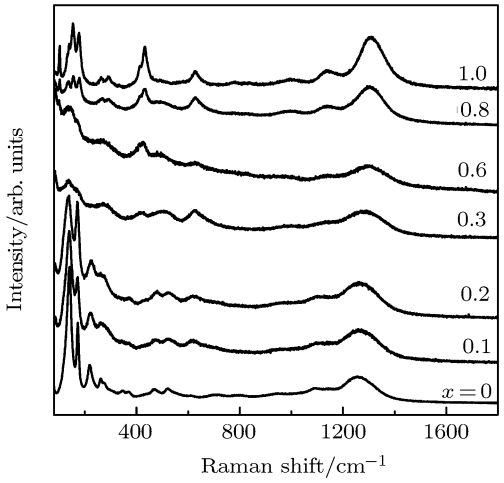


Fig. 2. Raman spectra for $Bi_{1-x}La_xFeO_3$ with $x = 0$, 0.1, 0.2, 0.3, 0.6, 0.8 and 1.0.

The second group includes the spectra with $x =$ 0.3 and 0.6. The most notable feature is the prominent decline of the intensities of the modes below 200 cm^{-1} and disappearance of the mode at around 250 cm^{-1}. Such a phenomenon suggests that the lattice structure for these two compounds undergoes dramatic changes. From a vibrational point of view, low frequency modes can be attributed as external modes due to the relative motion of A-site cations against the oxygen octahedrons. In the case of $BiFeO_3$, the A_1 modes in the low frequency range are closely associated with the Bi–O band.[19] It is natural that the intensity of the A_1 modes below 250 cm^{-1} declines due to the decrease in the percentage of the Bi–O band with large La substitution. Moreover, the overlapping of these modes reveals the increasing distortion and defects in the lattice due to the La substitution, which would also be responsible for the decrease of intensity.[23] In addition, the modes between 300 and 600 cm^{-1} merge into several broad bands. The increased structural disorder caused by the increasing substitution rate of La takes responsibility for this observation. Such a phenomenon also reveals the occurrence of the ferroelectric–paraelectric phase transition in this compound.[17] It is striking to find that the two modes at around 400 cm^{-1} appear and enhance gradually. These two peaks belong to the fingerprint peaks of the orthorhombic $LaFeO_3$.[24,25] The appearance of these two peaks indicates that the orthorhombic structure begins to emerge when the La

content increases to 0.3. The last group of spectra with $x = 0.8$ and 1.0 shows obvious spectral features of orthorhombic $LaFeO_3$. The broad bands below 400 cm^{-1} split into several sharp peaks, and a broad band appears in the spectral range of 400–500 cm^{-1}. It is noteworthy that the peak around 610 cm^{-1} shows enhancement, and the intensities of the two-phonon modes in the high frequency range increase simultaneously, especially the peak around 1300 cm^{-1}. The Raman results shown in Fig. 2 show good agreement with the XRD results (Fig. 1): the lattice structure for $Bi_{1-x}La_xFeO_3$ with $x \leq 0.2$ has rhombohedral symmetry, while the orthorhombic structure begins to appear in the range $0.2 < x \leq 0.6$. When $x \geq 0.8$, the orthorhombic structure is dominant and the lattice structure of $Bi_{1-x}La_xFeO_3$ is improved dramatically.

Compared with the spectra presented in Fig. 2, we find that the mode at around 610 cm^{-1} (P_{610}) and the two-phonon modes in the range of 900–1300 cm^{-1} exist in all $Bi_{1-x}La_xFeO_3$ compounds, although the other first-order Raman modes have changed significantly when the structure transforms from the rhombohedral to the orthorhombic phase. In order to analyse quantitatively the dependence of the Raman spectra for $Bi_{1-x}La_xFeO_3$ on the concentration of La, the Raman spectra are decomposed. Figure 3 presents the frequency shift and bandwidth of mode P_{610} as a function of the La doping concentration (x). It can be seen clearly that P_{610} shifts gradually to higher frequency positions with increasing La content. It is at 609.3 cm^{-1} for $BiFeO_3$ and at 627.9 cm^{-1} for $LaFeO_3$. However, on the other hand, the bandwidth of P_{610} behaves in a different way. It increases firstly and reaches the peak value of 56.8 cm^{-1} with $x = 0.3$. Then, it drops to 17.8 cm^{-1} with x=1.0.

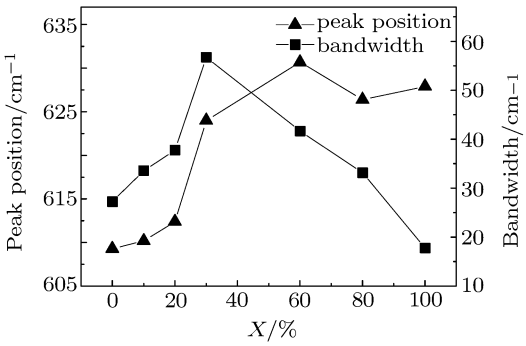


Fig. 3. Dependences of the frequency shifts and bandwidth of the peak at around 610 cm^{-1} on the La content.

The frequency shift and bandwidth of the two-phonon mode around 1250 cm^{-1} (P_{1250}) for all $Bi_{1-x}La_xFeO_3$ samples were plotted as a function of the La-doping concentration in Fig. 4. As shown in Fig. 4, the peak position of this band shifts continuously to higher frequency with increasing La content. It is at 1260.5 cm^{-1} for $BiFeO_3$ and 1309.4 cm^{-1} for $LaFeO_3$. On the other hand, the bandwidth of P_{1250} increases to the maximum value of 178.1 cm^{-1} at $x = 0.3$. From then on, the bandwidth decreases quickly with further increase of the La content, and reaches 118.7 cm^{-1} at $x = 1.0$, which is even smaller than that of pure $BiFeO_3$. It is noteworthy that the frequency shift and bandwidth of the fundamental mode P_{610} and its corresponding two-phonon mode P_{1250} behave in the same way (Figs. 3 and 4). The frequencies of the principal mode and corresponding higher order excitations increase with increasing La content in the $x = 0.1$, 0.2, 0.3 0.6 and 0.8 compounds. This hardening is likely to be attributed to the contraction of the unit cell, reflecting the increase in bond strength as Bi^{3+} is replaced by La^{3+}. In addition, a modulation in the system potential caused by the mass difference between Bi (208.98 g/mol) and La (138.9 g/mol) may also contribute to the energy shift.[26] The broadening of the Raman peaks with La content $x \leq 0.3$ is attributed to the increased lattice distortion arising from the competition between the rhombohedral and orthorhombic structure. When the orthorhombic structure becomes dominant ($x \geq 0.6$), the bandwidths of these peaks decline due to the improved lattice structure.

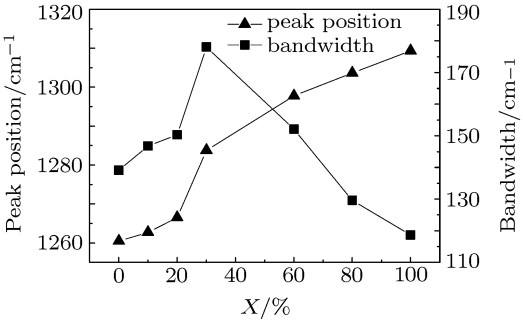


Fig. 4. Dependences of the frequency shifts and bandwidth of the peak near 1250 cm^{-1} on the La content.

Figure 5 displays the ratio of the integral intensity of peak P_{1250} to that of the whole spectra versus x. It can be seen clearly that the intensity proportion of peak P_{1250} gradually increases from 15% for $BiFeO_3$ to 38% for $LaFeO_3$. This is consistent with that shown in Fig. 2. With increasing La content, the two-phonon modes enhance, whereas the intensities of the first order phonons decrease simultaneously. The inset of

Fig. 5 presents the intensity ratio of peaks P_{1250} to $P_{610}(I_{1250}/I_{610})$ as a function of the La-doping concentration. The ratio I_{1250}/I_{610} drops quickly from 98.3 at $x = 0$ to 2.94 at $x = 0.3$. Then, it increases towards 7.85 when $x = 1$. As presented in Fig. 2, peak P_{610} enhances obviously with increasing La content. The ratio I_{1250}/I_{610} reaching the minimum value at $x = 0.3$ suggests the largest lattice distortion that arises from the appearance of the orthorhombic structure. From this point, the increase of I_{1250}/I_{610} indicates that the intensity of the peak P_{1250} undergoes a significant increase because of the increased spin-two-phonon coupling. The results presented in Fig. 5 are parallel with those shown in Figs. 3 and 4, indicating that the lattice structure of $Bi_{1-x}La_xFeO_3$ prefers the orthorhombic phase when $x > 0.3$. Although the lattice symmetry has transferred from the rhombohedral to the orthorhombic structure, the two-phonon peaks still exist and become even more intensive (Fig. 5).

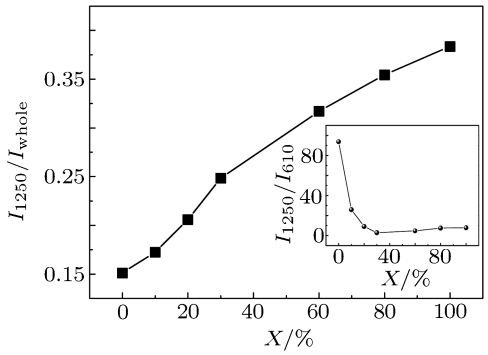


Fig. 5. Dependence of the integral intensity ratio of the peak at around 1250 cm^{-1} to the whole spectra on the La content. The inset shows the intensity ratio of the peak at 1250 cm^{-1} to the peak at 610 cm^{-1}.

This phenomenon reminds us that the intensive two-phonon peaks are widely observed in perovskite transition metal oxides.[24,25,27,28] Moreover, the intensive two-phonon peak is also observed in α-Fe_2O_3, which only contains FeO_6 octahedra.[29,30] The enhanced two-phonon peaks observed in $Bi_{1-x}La_xFeO_3$ may be tentatively associated with the strong spin-lattice coupling arising from the interaction between the adjacent magnetic sublattices. It is well known that La-doping will destroy the cycloidal spiral structure in $Bi_{1-x}La_xFeO_3$. $BiFeO_3$ exhibits weak magnetism at room temperature because of a residual moment from the canted spin structure, which can be released with La doping. When the substitution of La is increasing, the special magnetic properties disappear gradually, and the normal G-type antiferromagnetic ordering becomes the sole form. However, the coupling between the adjacent magnetic ions on the adjacent B-sites is increased as a result. Therefore, the enhanced two-phonon modes could be associated with the enhanced spin–lattice coupling owing to the La-doping. Our results suggest that the two-phonon modes are sensitive to the local structure, especially the sublattice of the magnetic ions on the B-sites, but insensitive to the macro-structure of the crystal.

4. Conclusion

In summary, XRD and Raman spectra for $Bi_{1-x}La_xFeO_3$ ($x = 0$, 0.1, 0.2, 0.3, 0.6, 0.8 and 1.0) are systematically studied. We find that the structure of $Bi_{1-x}La_xFeO_3$ changes from rhombohedral $BiFeO_3$ to orthorhombic $LaFeO_3$. The increase of the intensities of the peak around 610 cm^{-1} and the two-phonon modes in the range of 900–1300 cm^{-1} suggest that strong spin–lattice coupling exists in $Bi_{1-x}La_xFeO_3$. Moreover, the spin-two-phonon coupling seems to be enhanced with increasing La content, which is associated with the breakdown of the space modulated spin structure. All these results will be useful for understanding the correlation between the structural and magnetic properties of $Bi_{1-x}La_xFeO_3$.

References

[1] Hill N A 2000 *J. Phys. Chem.* B **104** 6694

[2] Eerenstein W, Mathur N D and Scott J F 2006 *Nature* **442** 759

[3] Ramesh R and Spaldin N A 2007 *Nat. Mater.* **6** 21

[4] Fischer P, Połomska M, Sosnowska I and Szymański M 1980 *J. Phys.* C **13** 1931

[5] Sosnowska I, Peterlin-Neumaier T and Steichele E 1982 *J. Phys.* C **15** 4835

[6] Yun K Y, Noda M and Okuyama M 2003 *Appl. Phys. Lett.* **83** 3981

[7] Qi X, Dho J, Tomov R, Blamire M G and MacManus-Driscoll J L 2005 *Appl. Phys. Lett.* **86** 062903

[8] Wang D H, Yan L, Ong C K and Du Y W 2006 *Appl. Phys. Lett.* **89** 182905

[9] Zavaliche F, Shafer P, Ramesh R, Cruz M P, Das R R, Kim D M and Eom C B 2005 *Appl. Phys. Lett.* **87** 252902

[10] Sun Y, Huang Z F, Fan H F, Ming X, Wang C Z and Chen G 2009 *Acta Phys. Sin.* **58** 0193 (in Chinese)

[11] Wang J, Neaton J B, Zheng H, Nagarajan V, Ogale S B, Liu B, Viehland D, Vaithyanathan V, Schlom D G, Waghmare U V, Spaldin N A, Rabe K M, Wuttig M and Ramesh R 2003 *Science* **299** 1719

[12] Zhang S T, Zhang Y, Lu M H, Du C L, Chen Y F, Liu Z G, Zhu Y Y, Ming N B and Pan X Q 2006 *Appl. Phys. Lett.* **88** 162901

[13] Cheng Z, Wang X, Dou S, Kimura H and Ozawa K 2008 *Phys. Rev.* B **77** 092101

[14] Singh V R, Garg A and Agrawal D C 2008 *Appl. Phys. Lett.* **92** 152905

[15] Wang Y, Zheng R Y, Sim C H and Wang J 2009 *J. Appl. Phys.* **105** 016106

[16] Haumont R, Kreisel J, Bouvier P and Hippert F 2006 *Phys. Rev.* B **73** 132101

[17] Yuan G L, Or S W and Chan L W 2007 *J. Phys.* D **40** 1196

[18] Singh M K, Jang H M, Ryu S and Jo M H 2006 *Appl. Phys. Lett.* **88** 042907

[19] Singh M K, Ryu S and Jang H M 2005 *Phys. Rev.* B **72** 132101

[20] Yang Y, Sun J Y, Zhu K, Liu Y L and Wan L 2008 *J. Appl. Phys.* **103** 093532

[21] Ramirez M O, Krishnamurthi M, Denev S, Kumar A, Yang S Y, Chu Y H, Saiz E, Seidel J, Pyatakov A P, Bush A, Viehland D, Orenstein J, Ramesh R and Gopalan V 2008 *Appl. Phys. Lett.* **92** 022511

[22] Yang Y, Sun J, Zhu K, Liu Y, Chen J and Xing X R 2009 *Physica* B **404** 171

[23] Dobal P S and Katiyar R S 2002 *J. Raman Spectrosc.* **33** 405

[24] Andreasson J, Holmlund J, Knee C S, Käll M, Börjesson L, Naler S, Bäckström J, Rübhausen M, Azad A K and Eriksson S G 2007 *Phys. Rev.* B **75** 104302

[25] Andreasson J, Holmlund J, Rauer R, Käll M, Börjesson L, Knee C S, Eriksson A K, Eriksson S G, Rübhausen M and Chaudhury R P 2008 *Phys. Rev.* B **78** 235103

[26] Zhu J, Mao X Y and Chen X B 2004 *Acta Phys. Sin.* **53** 3929 (in Chinese)

[27] Kruger R, Schulz B, Naler S, Rauer R, Budelmann D, Backstrom J, Kim K H, Cheong S W, Perebeinos V and Rubhausen M 2004 *Phys. Rev. Lett.* **92** 097203

[28] Perebeinos V and Allen P B 2001 *Phys. Rev.* B **64** 085118

[29] Martin T P, Merlin R, Huffman D R and Cardona M 1977 *Solid State Commun.* **22** 565

[30] Massey M J, Baier U, Merlin R and Weber W H 1990 *Phys. Rev.* B **41** 7822

[31] Chen J, Xing X R, Watson A, Wang W, Yu R, Deng J, Yan L, Sun C and Chen X 2007 *Chem. Mater.* **19** 3598